Novel Approach for Metallic Surface−Initiated Atom Transfer Radical Polymerization Using Electrografted Initiators Based on Aryl Diazonium Salts

ARTICLE *in* LANGMUIR · JUNE 2005

Impact Factor: 4.46 · DOI: 10.1021/la046912m · Source: PubMed

Novel Approach for Metallic Surface-Initiated Atom Transfer Radical Polymerization Using Electrografted Initiators Based on Aryl Diazonium Salts

Tarik Matrab,[†] Mohamed M. Chehimi,*[,†] Christian Perruchot,[†] Alain Adenier,[†] Alexandrine Guillez,[‡] Maud Save,[‡] Bernadette Charleux,[‡] Eva Cabet-Deliry,[§] and Jean Pinson[§,||]

ITODYS, UMR 7086 CNRS-Université Paris 7, 1 rue Guy de la Brosse, 75005 Paris, France, Laboratoire de Chimie Macromoléculaire, UMR 7610 CNRS-Université Paris 6, 4 Place Jussieu, 75252, Paris Cedex 05, France, and Laboratoire d'Electrochimie Moléculaire, UMR 75951 CNRS-Université Paris 7, 2 Place Jussieu, 75251, Paris Cedex 05, France

Received December 15, 2004. In Final Form: February 25, 2005

This paper reports on the preparation of poly(methyl methacrylate) (PMMA), poly(*n*-butyl acrylate) (PBA), and polystyrene (PS) brushes at the surface of conducting materials that were modified by the electrochemical reduction of a brominated aryl diazonium salt BF_4^-, $^+N_2-C_6H_4-CH(CH_3)-Br$ (**D1**). The grafted organic species $-C_6H_4-CH(CH_3)-Br$ was found to be very effective in initiating atom transfer radical polymerization (ATRP) of vinyl monomers. This novel approach combining diazonium salts and ATRP allowed PMMA, PBA, and PS brushes to be grown from the surface of iron electrodes. The polymer films were characterized in terms of their chemical structure by infrared reflection absorption spectroscopy and X-ray photoelectron spectroscopy. Atomic force microscopy studies indicated that the polymer brushes are densely packed. Contact angle measurements of water drops on PS and PMMA brushes were 88.1 ± 2.0 and 70.3 ± 2.1°, respectively, which is consistent with the published wettability data for the corresponding polymer sheets.

1. Introduction

Controlled radical polymerization (CRP)[1] can be achieved by a variety of modern approaches such as nitroxide-mediated processes,[2,3] reversible addition−fragmentation chain transfer,[4,5] and atom transfer radical polymerization (ATRP).[6,7] These methods are attractive because they ensure control over the molecular weight (MW) and molecular weight distribution (MWD) and allow the preparation of well-defined architectures. This contrasts with classical free radical polymerization which lacks control due to extensive irreversible termination reactions.

Particularly, ATRP has attracted the attention of several research teams[1,8,9] because it is applicable to a variety of functional monomers and can be performed at room temperature in either aqueous or organic solvents.[6,10] ATRP is also a very versatile method that leads to the formation of block copolymers, homopolymer brushes, mesoporous and interpenetrating networks, and so forth.[11] Recent progress in ATRP (and other CRPs) showed that it can be conducted in dispersed phase systems to produce colloidal polymer particles with controlled MWD and narrow particle size distribution.[10,12]

One important aspect of ATRP is that it can be initiated at the surface of flat substrates[13−18] or colloidal particles,[18−24] thus leading to the preparation of polymer brushes or hybrid organic/inorganic composite materials. In this regard, the substrate surfaces are first modified

† UMR 7086 CNRS-Université Paris 7.
‡ UMR 7610 CNRS-Université Paris 6.
§ UMR 75951 CNRS-Université Paris 7.
|| Present address: Alchimer, Z. I. La Bonde, 15 rue du Buisson aux Fraises, 91300 Massy, France.

(1) *Advances in Controlled/Living Radical Polymerization*; Matyjaszewski, K., Ed.; ACS Symposium Series 854; American Chemical Society: Washington, DC, 2003.
(2) Georges, M. K.; Veregin, R. P. N.; Kazmaier, P. M.; Hamer, G. P. *Macromolecules* **1993**, *26*, 2987.
(3) Hawker, C. J.; Bosman, A. W.; Harth, E. *Chem. Rev*. **2001**, *101*, 3661.
(4) Chong, Y. K.; Krstina, J.; Le, T. P. T.; Moad, G.; Postma, A.; Rizzardo, E.; Thang, S. H. *Macromolecules* **2003**, *36*, 2256.
(5) Chiefari, J.; Mayadunne, R. T. A.; Moad, C.; Moad, G.; Rizzardo, E.; Postma, A.; Skidmore, M. A.; Thang, S. H. *Macromolecules* **2003**, *36*, 2273.
(6) Matyaszewski, K.; Xia, J. *Chem. Rev*. **2001**, *101*, 2921.
(7) Kato, M.; Kamigaito, M.; Sawamoto, M.; Higashimura, T. *Macromolecules* **1995**, *28*, 1721.
(8) Matyaszewski, K., Ed. *Controlled Radical Polymerization*; American Chemical Society: Washington, DC, 1998; Vol. 685.
(9) Matyaszewski, K., Ed. *Controlled/Living Radical Polymerization: progress in ATRP, NMP and RAFT*; American Chemical Society: Washington, DC, 2000; Vol. 768.
(10) Qiu, J.; Charleux, B.; Matyjaszewski, K. *Prog. Polym. Sci.* **2001**, *26*, 2083.
(11) Pyun, J.; Matyjaszewski, K. *Chem. Mater*. **2001**, *13*, 3436.
(12) Cunningham, M. F. *Prog. Polym. Sci.* **2002**, *27*, 1039.
(13) Kim, J.-B.; Bruenig, M. L.; Baker, G. L. *J. Am. Chem. Soc*. **2000**, *122*, 7616.
(14) Jones, D. M.; Smith, J. R.; Huck, W. T. S.; Alexander, C. *Adv. Mater.* **2002**, *14*, 1130.
(15) Desai, S. M.; Solanky, S. S.; Mandale, A. B.; Rathore, K.; Singh, R. P. *Polymer* **2003**, *44*, 7645.
(16) Mori, H.; Müller, A. H. E. *Top. Curr. Chem.* **2003**, *228*, 1.
(17) (a) Ejaz, M.; Ohno, K.; Tsujii, Y.; Fukuda, T. *Macromolecules* **2000**, *33*, 2870. (b) Ejaz, M.; Yamamoto, S.; Ohno, K.; Tsujii, Y.; Fukuda, T. *Macromolecules* **1998**, *31*, 5934.
(18) Edmondson, S.; Osborne, V. L.; Huck, W. T. S. *Chem. Soc. Rev.* **2004**, *33*, 14.
(19) Guerrini, M. M.; Charleux, B.; Vairon J.-P. *Macromol. Rapid Commun.* **2000**, *21*, 669.
(20) Pyun, J.; Kowalewski, T.; Matyaszewski, K. *Macromol. Rapid Commun.* **2003**, *24*, 1043.
(21) Chen, X.; Randall, D. P.; Perruchot, C.; Watts, J. F.; Patten, T. E.; von Werne, T.; Armes, S. P. *J. Colloid Interface Sci.* **2003**, *257*, 56.
(22) Kim, D. J.; Heo, J. Y.; Kim, K. S.; Choi, I. S. *Macromol. Rapid Commun.* **2003**, *24*, 517.
(23) von Werne, T.; Patten, T. E. *J. Am. Chem. Soc*. **1999**, *121*, 7409.
(24) Carrot, G.; Diamanti, S.; Manuszak, M.; Charleux, B.; Vairon, J. P. *J. Polym. Sci., Part A: Polym. Chem*. **2001**, *39*, 4294.

10.1021/la046912m CCC: $30.25
Published on Web 03/29/2005

with specific coupling agents, such as silanes for silica surfaces, bearing functional groups that are able to initiate ATRP of styrene, (meth)acrylates, and other monomers.[16] Alternative surface-initiated ATRP methods consist in employing initiator-terminated thiols,[13,14] photo-brominated polymer surfaces,[15] a reactive 2-bromopropionyl bromide,[22] or a macroinitiator.[25,26] These few examples clearly show that surface-initiated ATRP is very versatile and can be achieved by a variety of ways depending on the nature of the substrate that serves for the growth of linear or (hyper)branched polymer brushes.

Since the early 1990s, it has been shown that carbon, metallic, and semiconductor surfaces can be modified by the electrochemical reduction of aryl diazonium salts (see Scheme 2).[27] This has been confirmed by other research groups both on carbon and on metallic surfaces.[28−33]

By choosing the appropriate diazonium salt (with, e.g., 4-benzoylphenyl moieties), polystyrene (PS) was attached to the modified iron surface and covalently bound under irradiation.[27i] Alternatively, carboxyphenyl groups were attached to the iron surface by reduction of the diazonium salt of 4-aminobenzoic acid, and the subsequent grafting of poly(1,2-propanediyl fumarate) to the phenylcarboxylate functions was achieved through ionic bonds with Mg^{2+} ions.[27i]

Diazonium salts were found to be effective in immobilizing colloidal gold nanoparticles[34] onto carbon surfaces or in the preparation of a modified carbon electrode that exhibits a redox electroactivity that is due to 4-aminophenyl ferrocene grafted to the former electrode.[31c] Polyoxometalates were attached as catalysts on the surface of carbon through coupling with diazonium salts.[30] In the biomedical domain, diazonium salts were employed in view of preparing biotinylated reactive surfaces.[32]

Because aryl diazonium salts appear to be versatile coupling agents for the modification of surfaces,[27i,34] we wished to explore their propensity to surface-initiate a CRP, namely, ATRP.

Scheme 1. Comparison of the Chemical Structures of a Bulk Solution ATRP Initiator and Its Diazonium Salt Analogue (D1)

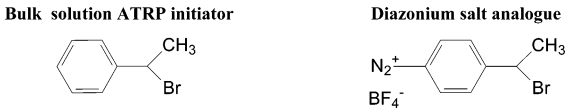

Actually, CRP of styrene has already been initiated from electrografted poly(functional alkyl acrylate) onto steel by the research team led by Jerôme. This *grafting from* method combines an electrochemical surface modification with ATRP of styrene[26] or nitroxide-mediated copolymerization of styrene with 2-(dimethylamino ethyl)acrylate.[35] The same research group extended CRP to the surface-initiated ring-opening polymerization of ϵ-caprolactone on steel.[36]

As far as we are concerned, the rationale for using specific diazonium salts to initiate ATRP is that they readily attach to the surface of carbon, metals, and other conductors via covalent bonding, as recently demonstrated by X-ray photoelectron spectroscopy (XPS).[37] Moreover, some ATRP initiators have chemical structures that resemble those of diazonium salts, with the sole difference being that they lack the $-N_2^+$ group. Scheme 1 shows the chemical structure of one diazonium salt with its corresponding ATRP initiator. Actually, the brominated aryl diazonium salt BF_4^-, $^+N_2-C_6H_4-Br$ has already been reduced electrochemically and attached to carbon felt.[27j] It is, thus, likely that the brominated diazonium salt **D1** shown in Scheme 1 undergoes similar electrochemical reduction.

Bearing in mind the literature precedent, it became clear to us that ATRP was very likely to be initiated at the surface of conducting substrates such as carbon and metals modified by the now well-established electrochemical reduction of specific aryl diazonium salts.

The aim of this paper is to offer a novel approach based on diazonium salts for initiating ATRP of methyl methacrylate (MMA), *n*-butyl acrylate (BA), and styrene at the surface of iron in the presence of Cu(I)/Cu(II) catalyst. The metallic substrate served as the working electrode material for the electrochemical reduction of the novel aryl diazonium salt, namely, BF_4^-, $^+N_2-C_6H_4-CH(CH_3)-Br$ (**D1**), and polymer brushes were expected to grow from the brominated iron surface sites.

Iron was chosen, rather than carbon or gold, because of its nearly universal use as an industrial metal and the need to protect its surface from corrosion in nearly all practical applications. Surface polymerization of hydrophobic monomers[27h−j] could be a means to protect the surface. The anti-orrosion effect of these polymer-grafted overlayers will be reported elsewhere.

The set of reactions for the surface modification of iron by the electrochemical reduction of brominated aryl diazonium salts and the subsequent surface-initiated ATRP of a vinylic monomer is summarized in Scheme 2.

This *grafting from* method was performed in the presence or absence of the sacrificial ATRP initiator (1-phenylethyl bromide, 1-PEBr) added in solution. The use of the sacrificial initiator was aimed at increasing the

(25) Chen, X.; Armes, S. P. *Adv. Mater.* **2003**, *15*, 1558.
(26) Claes, M.; Voccia, S.; Detrembleur, C.; Jérôme, C.; Gilbert, B.; Leclère, Ph.; Geskin, V. M.; Gouttebaron, R.; Hecq, M.; Lazzaroni, R.; Jérôme, R. *Macromolecules* **2003**, *36*, 5926.
(27) (a) Delamar, M.; Hitmi, R.; Pinson, J.; Savéant, J. M. *J. Am. Chem. Soc*. **1992**, *114*, 5883. (b) Bourdillon, C.; Delamar, M.; Demaille, C.; Hitmi, R.; Moiroux, J.; Pinson, J. *J. Electroanal. Chem.* **1992**, *336*, 113. (c) Allongue, P.; Delamar, M.; Desbat, B.; Fagebaume, O.; Hitmi, R.; Pinson, J.; Savéant, J. M. *J. Am. Chem. Soc.* **1997**, *119*, 201. (d) Delamar, M.; Desarmot, G.; Fagebaume, O.; Hitmi, R.; Pinson, J.; Savéant, J. M. *Carbon* **1997**, *36*, 801. (e) Henry de Villeneuve, C.; Pinson, J.; Bernard, M. C.; Allongue, P. *J. Phys. Chem. B* **1997**, *101*, 2415. (f) Allongue, P.; Henry de Villeneuve, C.; Pinson, J.; Ozanam, F.; Chazalviel, J. N.; Wallart, X. *Electrochim. Acta* **1998**, *43*, 2791. (g) Adenier, A.; Bernard, M. C.; Chehimi, M. M.; Cabet-Deliry, E.; Desbat, B.; Fagebaume, O.; Pinson, J.; Podvorica, F. *J. Am. Chem. Soc*. **2001**, *123*, 4541. (h) Chaussé, A.; Chehimi, M. M.; Karsi, N.; Pinson, J.; Podvorica, F.; Vautrin-Ul, C. *Chem. Mater.* **2002**, *14*, 392. (i) Adenier, A.; Cabet-Deliry, E.; Lalot, T.; Pinson, J.; Podvorica, F. *Chem. Mater.* **2002**, *14*, 4576. (j) Coulon, E.; Pinson, J.; Bourzat, J.-D.; Commerçon, A.; Pulicani, J.-P. *J. Org. Chem.* **2002**, *67*, 8513.
(28) Downard, A. J. *Electroanalysis* **2000**, *12*, 1085.
(29) Kariuki, J. K.; McDermott, M. T. *Langmuir* **1999**, *15*, 6534.
(30) Liu, S.; Tang, Z.; Shi, Z.; Wang, E.; Dong, S. *Langmuir* **1999**, *15*, 7268.
(31) (a) Saby, C.; Ortiz, B.; Champagne, G. Y.; Bélanger, D. *Langmuir* **1997**, *13*, 6805. (b) Ortiz, B.; Saby, C.; Champagne, G. Y.; Bélanger, D. *J. Electroanal. Chem.* **1998**, *455*, 75. (c) Ghodbane, O.; Chamoulaud, G.; Bélanger, D. *Electrochem. Commun.* **2004**, *6*, 254.
(32) Dequaire, M.; Degrand, C.; Limoges, B. *J. Am. Chem. Soc.* **1999**, *121*, 6946.
(33) (a) Liu, Y.-C.; McCreery, R. L. *J. Am. Chem. Soc*. **1995**, *117*, 11254. (b) Ray, K., III; McCreery, R. L. *Anal. Chem*. **1997**, *69*, 4680. (c) DuVall, S. H.; McCreery, R. L. *Anal. Chem*. **1999**, *71*, 4594. (d) Ranganathan, S.; Steidel, I.; Anariba, F.; McCreery, R. L. *Nano Lett*. **2001**, *1*, 491. (e) Solak, A. O.; Eichorst, L. R.; Clark, W. J.; McCreery, R. L. *Anal. Chem.* **2003**, *75*, 296. (f) Hurley, B.; McCreery, R. L. *J. Electrochem. Soc*. **2004**, *151*, B252.
(34) Harnisch, J. A.; Pris, A. D.; Porter, M. D. *J. Am. Chem. Soc.* **2001**, *123*, 5829.
(35) Ignatova, M.; Voccia, S.; Gilbert, B.; Markova, N.; Mercuri, P. S.; Galleni, M.; Sciannamea, V.; Lenoir, S.; Cossement, D.; Gouttebaron, R.; Jérôme, R.; Jérôme, C. *Langmuir* **2004**, *20*, 10718.
(36) Voccia, S.; Bech, L.; Gilbert, B.; Jérôme, R.; Jérôme, C. *Langmuir* **2004**, *20*, 10670.
(37) Boukerma, K.; Chehimi, M. M.; Pinson, J.; Blomfield, C. *Langmuir* **2003**, *19*, 6333.

Scheme 2

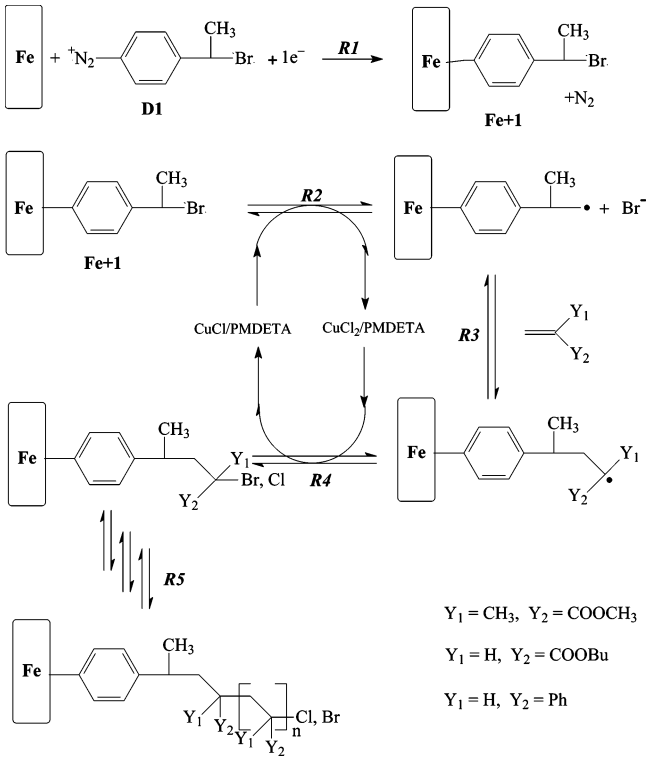

Scheme 3

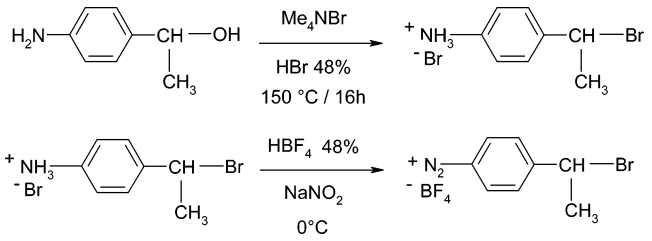

concentration of the Cu^{II} complex, to better control the polymerization,[17b] whereas its absence permitted checking whether radical polymerization from the surface alone would provide the electrochemically treated metal surfaces with the same quality of polymer coating. The polymer coatings were characterized by means of infrared reflection absorption spectroscopy (IR-RAS), XPS, atomic force microscopy (AFM), and measurements of static contact angles of water drops. Poly(methyl methacrylate) (PMMA), poly(*n*-butyl acrylate) (PBA), and PS bulk powders prepared by ATRP served as reference materials.

2. Experimental Section

2.1. Synthesis of the Diazonium Salt $^{+}N_2-C_6H_4-CH(CH_3)-Br$. The starting diazonium salt **D1** was synthesized in one pot from the commercially available 1-(4-aminophenyl)-ethanol (1 g) by heating at 150 °C in 48% HBr (5 mL) for 16 h, then cooling to 0 °C (Scheme 3) to give a yellow precipitate. The diazotization is then achieved by the standard method that consists of adding HBF_4 and $NaNO_2$. The precipitated brown diazonium tetrafluoroborate was filtered and washed with 5% $NaBF_4$, methanol, and ether (cf. characterization by IR in Results and Discussion).

2.2. Preparation and Electrochemical Treatment of Iron Plates. Iron disks (1-cm diameter, Weber Métaux) were carefully polished down to 1 μm with diamond paste and rinsed under sonication in deaerated acetone to prevent any oxidation of the surface. On iron, the reduction wave of **D1** is too positive to be observed before the oxidation of iron. Grafting was achieved by chronoamperometry for 300 s, at a potential 300 mV negative to the peak potential (measured on carbon), and at this potential iron is not oxidized. The iron disks were then thoroughly rinsed under sonication in deaerated acetone.

2.3. Surface-Initiated ATRP. The electrochemically pretreated iron disks were coated with PS, PMMA, and PBA grown by surface-initiated ATRP. The MMA, BA, and styrene (Aldrich) were each distilled prior to polymerization. *N*,*N*,*N*′,*N*″,*N*″-Pentamethyldiethylenetriamine (PMDETA), CuBr, CuCl, and $CuCl_2$ (Aldrich) were used as received for the catalysis of the surface-initiated ATRP. Surface-initiated ATRP was undertaken with and without sacrificial initiator in solution. When used, the sacrificial initiator was 1-PEBr (Aldrich, used as received).

A typical styrene polymerization procedure is as follows. First, a 100-mL Schlenk flask equipped with a magnetic stir bar and sealed with a rubber septum was deoxygenated by a vacuum followed by back-filling with nitrogen three times. The CuBr powder (71 mg, 4.9×10^{-4} mol) and the iron disk were introduced into the flask under a nitrogen flow. A mixture containing styrene (36 g, 3.46×10^{-1} mol), 1-PEBr (94 mg, 5.1×10^{-4} mol), and PMDETA (84 mg, 4.7×10^{-4} mol), previously degassed, was added the polymerization flask using a double-tipped needle under a nitrogen flow. The flask was placed in an oil bath at 100 °C for 16 h. The polymerization was stopped by cooling and opening the flask to expose the catalyst to air. The reaction mixture was then diluted in methylene chloride and passed through a column filled with neutral alumina to remove the copper complex. The polymer was precipitated in excess ethanol, and the molar masses were analyzed by size exclusion chromatography (SEC; $M_n = 54\,800$ g/mol, $M_w/M_n = 1.21$). For the MMA and the BA polymerization, the reaction flask was equipped with a condenser, and the following procedure was the same. Conversions were determined by ^1H NMR analysis of the crude samples in $CDCl_3$.

Because it was important to genuinely confirm the graft polymerization by surface-initiated ATRP using aryl diazonium salts, the modified iron disks were systematically rinsed after the polymerization reaction in dichloromethane under sonication for five periods of 5 min. This thorough rinsing was aimed at removing any physisorbed polymer chains that have been synthesized in solution without any anchoring site on the metal surface.

2.4. Analytical Techniques for Polymer Characterization. The average molar mass and molar mass distribution of the copolymers were obtained by SEC in tetrahydrofuran (THF) with a 1 mL min^{-1} flow rate. The apparatus was composed of three linear columns (3 PSS SDV 8 × 300 mm, 5 μm) thermostated at 40 °C and two detectors: RI (LDC Analytical, refractor Monitor IV) and UV operating at 254 nm (Waters 484). The sample concentrations were 5 mg/mL. The molar masses were calculated from a calibration curve based on PS standards. On the basis of the Mark−Houwink Sakurada (MHS) parameters, the PS calibration is appropriate for the PBA but a multiplication factor of 1.3 was applied to calculate accurate PMMA molar masses. Indeed, the MHS parameters in THF at 25 °C are the following: $K_{PS} = 11.7 \times 10^{-5}$ dL g^{-1} and $\alpha_{PS} = 0.717$ for PS,[38] $K_{PBA} = 11.8 \times 10^{-5}$ dL g^{-1} and $\alpha_{PBA} = 0.716$ for PBA,[39] and $K_{PMMA} = 12.3 \times 10^{-5}$ dL g^{-1} and $\alpha_{PMMA} = 0.689$ for PMMA.[40]

^1H NMR (250 MHz) spectra of the crude polymers were performed in $CDCl_3$ in 5-mm tubes at room temperature using a AC250 Bruker spectrometer.

2.5. IR-RAS. All infrared absorption spectra were recorded on a Magna-860 Fourier transform infrared spectrometer (Nicolet Instrument Corp., Madison, WI, U.SA.), at a 4-cm^{-1} spectral resolution.

The transmittance absorption spectrum of the diazonium salt **D1** in a KBr pellet was performed using a standard DTGS detector and by collecting 50 scans.

Plates of grafted **Fe**+**1** and **Fe**+**1**+**PMMA** were analyzed by IR-RAS, using an 80° incidence angle accessory and a high-sensitivity mercury cadmium telluride (MCT-A/4000-625 cm^{-1})

(38) Kolinsky, M.; Janca, J. *J. Polym. Sci., Polym. Chem. Ed.* **1974**, *12*, 1181.

(39) Schmidtt, B. Ph.D. Thesis, Universität Mainz, Mainz, Germany, 1999.

(40) Mori, S., Barth, H. G., Eds. *Size Exclusion Chromatography*; Springer-Verlag: New York, 1999.

detector. To improve the signal-to-noise ratio, **Fe+1** and **Fe+1+PMMA** spectra were recorded by collecting 1000 scans. All spectra were baseline-corrected using OMNIC 6.1 internal software and were unsmoothed.

2.6. XPS. XPS spectra were recorded using a Thermo VG Scientific ESCALAB 250 system fitted with a micro-focused, monochromatic Al Kα X-ray source (1486.6 eV) and a magnetic lens which increases the electron acceptance angle and, hence, the sensitivity. An X-ray beam of 650-μm size was used at a power of 10 mA × 15 kV. The spectra were acquired in the constant analyzer energy mode, with a pass energy of 150 and 40 eV for the survey and the narrow regions, respectively. In addition, ultimate spectral resolution was achieved for the C(1s) regions by setting the pass energy at 10 or 15 eV. Because this machine produces spectra with very high signal-to-noise ratios, it was found to be appropriate for recording valence band spectra with relatively high counts with a pass energy set at 20 eV. The Avantage software, version 1.85, was used for digital acquisition and data processing. Spectral calibration was determined by setting the aliphatic C−C/C−H C(1s) peak at 285 eV. The surface composition was determined using the manufacturer's sensitivity factors. The fractional concentration of a particular element A (% A) was computed using

$$\%\mathrm{A} = \frac{I_\mathrm{A}/S_\mathrm{A}}{\sum(I_\mathrm{n}/S_\mathrm{n})} \times 100$$

where I_n and S_n are the integrated peak areas and the sensitivity factors, respectively.

Some surface analysis measurements were also performed using the Surface Science Instrument (SSI) spectrometer, SSX 100 model, equipped with a monochromatic Al Kα X-ray source (1486.6 eV). The X-ray spot size was 1000 μm. The pass energy was set at 150 and 100 eV for the survey and the narrow scans, respectively. The step size was 1.12 eV for the survey spectrum and 0.096 eV for the high-resolution spectra.

2.7. AFM. Untreated, electrochemically modified and polymer-coated iron disks were imaged by a Nanoscope III Digital Instrument in the tapping mode using a Si_3N_4 tip cantilever. The cantilever oscillation frequency was set at 320 kHz. Tips of the cantilever were characterized by the radius of their curvature, which was equal to 7 ± 2 nm. No computer filtering procedure was used to treat the images. Tapping mode imaging was recorded with 256 pixels per line with a scan rate of 1.2 Hz. Surface roughness (R_a) was determined at the same scale (1 μm) for each sample.

2.8. Contact Angle Measurements. Water drop static contact angles were measured using a RAME HART NRL goniometer (model 100-00) equipped with a microscope and illumination system to visualize both the drop deposited on the plates and the measurement marker. The plates were placed on a flat, horizontal support in a chamber that was thermostated at 20 °C. Contact angles from both apparent ends (left and right) were considered and usually found to be equal within standard error. Drops of 2−3 μL of distilled water were used. Static contact angles were the average values of at least six measurements.

3. Results and Discussion

The cyclic voltametry of **D1** was conducted on a glassy carbon electrode to determine its reduction potential. Indeed, the voltammogram of **D1** cannot be observed on an iron electrode as its peak potential is positive to the onset of the oxidation of iron. Figure 1 shows the cyclic voltametry of **D1** on a glassy carbon electrode in acetonitrile (ACN) + 0.1 M NBu_4BF_4. One can observe a broad, irreversible, monoelectronic wave at $Ep_c = -0.31$ V/saturated calomel electrode (SCE) which corresponds to the reduction of the diazonium salt. The electron transfer is concerted with the cleavage of dinitrogen,[27h] giving an aryl radical which binds to the surface according to reaction R1.[27c] Upon repetitive scanning, this wave decreases to negligible values, as usually observed with diazonium

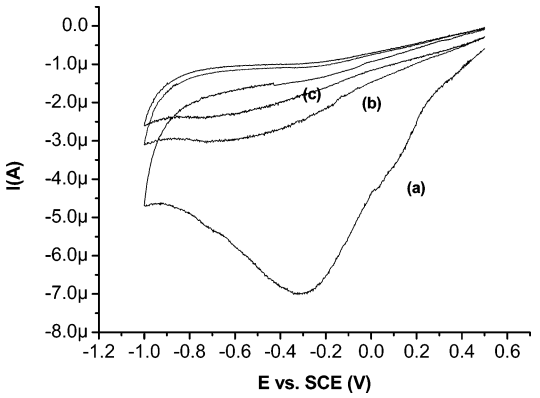

Figure 1. Cyclic voltammogram of a carbon electrode grafted with **D1** in ACN + 0.1 M NBu_4BF_4: (a) first, (b) second, and (c) third cycles, $v = 0.2$ V s^{-1}. Reference SCE.

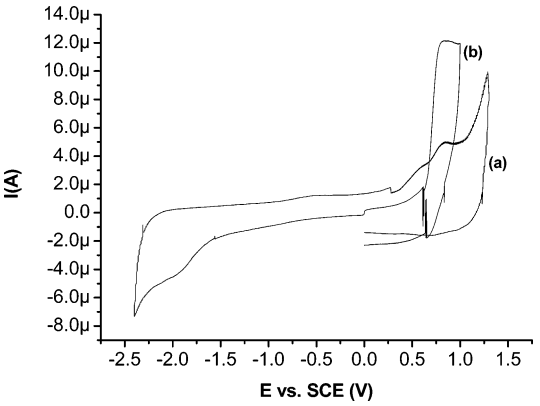

Figure 2. Cyclic voltammogram of (a) a carbon electrode grafted with **1** in ACN + 0.1 M NBu_4BF_4 and (b) a solution of NEt_4Br (1 mM) on a carbon electrode. $v = 0.2$ V/SCE. Reference SCE.

Scheme 4

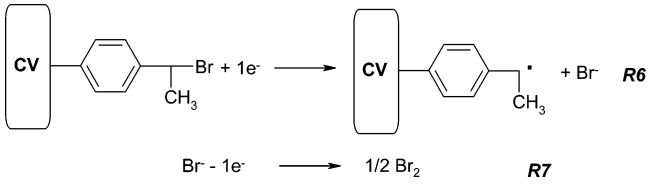

salts; this decrease corresponds to the formation of the organic layer on top of the electrode surface.[27,28,31,33] That the electrografting of the bromo initiator has indeed taken place on the surface of carbon was checked as shown in Figure 2. As the potential of the modified carbon electrode (Figure 2a) is scanned, a reduction wave is observed at ∼−2.0 V/SCE; this wave corresponds to the reduction of the benzylic −C−Br bond of the bonded initiator (Scheme 4). On the anodic scan, one observes at +0.6 V/SCE the oxidation wave of the liberated bromide ion. That this peak corresponds to the oxidation of a bromine ion is supported by the fact that NEt_4Br shows a peak at the same potential (Figure 2b). On iron plates grafting was achieved by chronoamperometry (Figure 3) maintaining for 300 s a 300-mV negative potentiel relative to the peak potential measured on carbon. The very steep decrease of the current with time is, again, characteristic of the formation of the organic layer which blocks the electron transfer from the electrode. The iron disks were then thoroughly rinsed under sonication in deaerated acetone.

As will be demonstrated below by means of IR-RAS and XPS, the attachment of the 1-(bromoethyl)benzene group

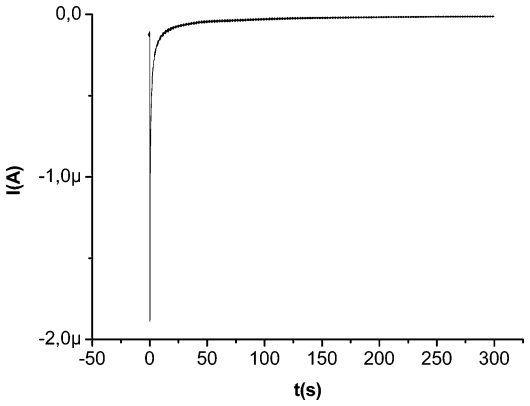

Figure 3. Chronoamperometry of an iron disk grafted with **D1** in ACN + 0.1 M NBu_4BF_4, t = 300 s, v = 0.2 V s^{-1}. Reference SCE.

(**1**) to the iron surface has taken place to give **Fe**+**1**. This electrografted organic species is not removed by sustained ultrasonic rinsing.

The iron disks treated by the electrochemical reduction of **D1** (**Fe**+**1**) were subjected to ATRP[11] conditions to grow polymer brushes from the surface. The surface-initiated ATRP of MMA, BA (see Scheme 2), and styrene should lead to PMMA, PBA, and PS, respectively. **Fe**+**1** iron disks were treated under the typical experimental conditions (with and without sacrificial initiator in solution) reported in Table 1. The end-coated iron plates are abbreviated by **Fe**+**1**+**PMMA**, **Fe**+**1**+**PBA**, and **Fe**+**1**+**PS**. The abbreviations followed by an asterisk (*) correspond to specimens prepared with 1-PEBr used as a sacrificial initiator (e.g., **Fe**+**1**+**PMMA***).

Several studies on ATRP from an inorganic surface showed that the average molar mass and the polydispersity of the grafted polymer are practically the same as the values obtained for the soluble polymer formed in bulk solution from the added free initiator.[17,41] The absence of any hydrolytic bond between the metallic surface and the macromolecular chains imparts good chemical stability but prevents de-grafting and, hence, the direct analysis of the grafted polymer. Consequently, the recovered nongrafted polymer chains will serve as a reference for the characterization of the grafted polymer chains. The linearity of the logarithmic monomer concentration versus time indicated minimal termination reactions (Figure 4). Moreover, the linear increase of the molar mass versus conversion and the low polydispersity indexes (M_w/M_n < 1.21) indicate a reasonable control of the polymerization (Figure 5).

For BA and MMA polymerizations, the experimental molar masses are higher than those calculated using

$$\mathrm{DP} = ([\mathrm{M}]_0 - [\mathrm{M}]_t)/[\mathrm{In}]_0$$

where DP is the degree of polymerization, $[M]_0$ is the initial monomer concentration, $[M]_t$ is its concentration at time t, and $[In]_0$ is the initiator initial concentration.

To obtain, for a given monomer, experimental M_n values (determined by SEC in this work) matching the theoretical ones, it is necessary to consider carefully several parameters including the initiator structure, the initiator/catalyst system, the solvent, and the polymerization temperature.[6] In the present work, the working temperature used is equal or close to the recommended one for the ATRP of styrene, MMA, and BA[6] and can, thus, not account for the discrepancy between the target and the experimental DP of PMMA and PBA.

The halogenated initiator must preferably have a chemical structure resembling that of the growing chains.[6] 1-PEBr is, thus, a recommended initiator for the ATRP styrene in terms of control of DP, and this is indeed the case of the present work (see Table 1, entry 1, and Figure 5a). Although benzyl-substituted halides can be inefficient for the ATRP of methacrylates,[6] under certain conditions the 1-PEBr/CuCl system was found very convenient for the control of the MMA polymerization.[42] This result was interpreted in terms of the halogen exchange concept.

For PBA, Table 1 reports also higher experimental DP than the theoretically expected one, perhaps due to the use of an initiator that does not have a similar chemical structure. However, very recently it has been shown that combining the 1-PEBr/CuBr system with a new TREN-based ligand resulted in a PBA with comparable theoretical and experimental M_n with a polydispersity of 1.21 for a conversion rate of 58%.[43]

The solvent is another important parameter affecting the experimental M_n values. In this work, toluene, a weakly polar solvent, was used which yields a lower solubility of the CuCl and, thus, a lower initiation catalysis. It follows that propagation is faster than initiation and the experimental M_n obtained is higher than the theoretical one. An attempt to increase the polarity of the solvent[44] by mixing toluene with dimethylformamide (10%, v/v) resulted indeed in comparable experimental and calculated M_n values. However, for unknown reasons, the iron disks appeared slightly corroded. We were then left with the 1-PEBr/CuCl system in pure toluene.

Although it was difficult to meet all the requirements for obtaining comparable theoretical and experimental DP values for all monomers used in this work, the systems used in this work permitted, nevertheless, polydispersity indices lower than 1.21 to be obtained.

Figure 6 presents the IR-RAS spectra of **Fe**+**1** and the KBr pellet IR spectrum of **D1**. First, the spectrum of **Fe**+**1** lacks the band at 2258 cm^{-1} characteristic of the N_2^+ group, which indicates that the diazonium salt **D1** has indeed been reduced and grafted on the iron plate, rather than merely being physisorbed. The peaks centered at 1579 and 1508 cm^{-1} (ring vibrations) are characteristic of the aromatic ring, 1083 cm^{-1} (in-plane CH vibrations), and 834, 793, and 700 cm^{-1} (out-of-plane CH vibrations).

Selected IR-RAS spectra are shown in Figure 7 to track the changes in the surface chemistry of **Fe**+**1** by the grafted PMMA.

The IR-RAS spectrum of **Fe**+**1**+**PMMA*** (Figure 7a) exhibits a striking difference by comparison to the uncoated **Fe**+**1** in that it has a very sharp C=O stretch at 1735 cm^{-1} which is characteristic of the ester carbonyl group of polymethacrylates and polyacrylates. The complex bands centered at 1155 and 1267 cm^{-1} are characteristic of the C—O stretching vibrations. The convoluted peaks centered at 1452 cm^{-1} are due to the $-CH_2-$ and $C-CH_3$ deformation.

In Figure 7b the IR-RAS spectrum of **Fe**+**1**+**PMMA** exhibits a quasi-identical spectrum compared to that in Figure 7a, however, with less intense C=O and the other bands discussed above. This lower intensity of the IR-

(41) Husseman, M.; Malmström, E. E.; McNamara, M.; Mate, M.; Mecerreyes, D.; Benoît, D.; Hedrick, J. L.; Mansky, P.; Huang, E.; Russell, T. P.; Hawker, C. J. *Macromolecules* **1999**, *32*, 1424.

(42) Matyjaszewski, K.; Wang, J.-L.; Grimaud, T.; Shipp, D. A. *Macromolecules* **1998**, *31*, 1527.

(43) Gromada, J.; Spanswick, J.; Matyjaszewski, K. *Macromol. Chem. Phys.* **2004**, *205*, 551.

(44) Matyjaszewski, K.; Nakagawa, Y.; Jasieczek, C. B. *Macromolecules* **1998**, *31*, 1535.

Table 1. Synthesis of PS, PMMA, and PBA by ATRP Using Various Experimental Conditions

expt	monomer	[M]^a (mol L^{-1})	CuX/CuX$_2$	[M]$_0$:[1-PEBr]$_0$:[CuCl]$_0$:[CuCl$_2$]:[PMDETA]$_0$^{b}	T (°C)	time (min)	conv	$\bar{M}_n$ theor^b (g/mol)	$\bar{M}_n$ SEC (g/mol)	$\bar{M}_w/\bar{M}_n$
1	styrene	8.7	CuBr	681:1:1:0:1	100	960	0.78	55 500	54 800	1.21
2	BA	5.8	CuCl/CuCl$_2$	120:1:0.45:0.05:0.5	90	210	0.88	13 700	24 100	1.08
3	BA	5.8	CuCl/CuCl$_2$	120:0:0.45:0.05:0.5	90	210	0.88			
4	MMA	4.8	CuCl/CuCl$_2$	200:1:0.33:0.17:0.5	90	184	0.43	8800	19 300	1.16
5	MMA	4.8	CuCl/CuCl$_2$	200:0:0.33:0.17:0.5	90	184	0.43			
6	MMA	4.7	CuCl/CuCl$_2$	700:1:0.9:0.1:1	90	360	0.40	28 000	53 700	1.12

^{a} Polymerizations were carried out in the bulk for styrene monomer and in toluene for BA and MMA monomers. ^{b} [1-PEBr]$_0$ is the concentration of the free added initiator. We neglected the concentration of the initiator grafted on the iron disk.

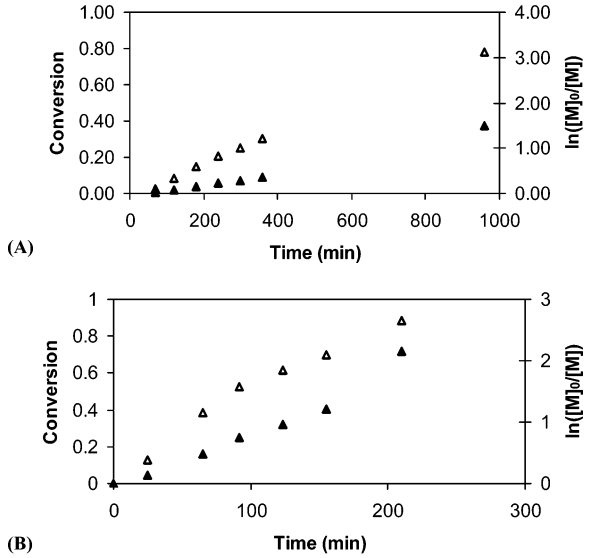

Figure 4. Time-conversion plots (△) and first-order kinetic plots (▲) for the ATRP of styrene (A) and BA (B) initiated by 1-PEBr with the catalyst Cu(I)/PMDETA, in the presence of the grafted iron disks. See experiments 1 and 2 in Table 1 for the experimental conditions.

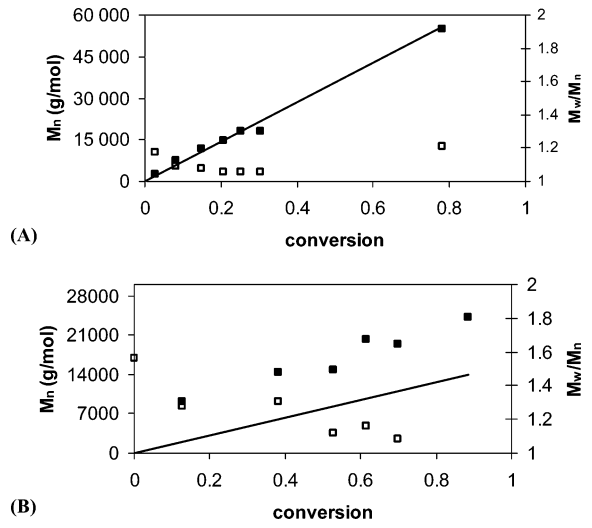

Figure 5. Dependence of molar mass, M_n (■), and polydispersity, M_w/M_n (□), on monomer conversion for the ATRP of styrene (A) and BA (B) initiated by 1-PEBr with the catalyst Cu(I)/PMDETA, in the presence of the grafted iron disks. See experiments 1 and 2 in Table 1 for the experimental conditions. The full line corresponds to the theoretical M_n.

RAS bands is perhaps linked to the efficiency of the sacrificial initiator in obtaining dense polymer overlayers. Nevertheless, since PMMA brushes grow from **Fe+1** without the support of any sacrificial initiator in solution, the brominated diazonium salts appear to be very effective for surface-initiated ATRP; the use of added 1-PEBr is beneficial only for the better control of the growth and length of the polymer chains.

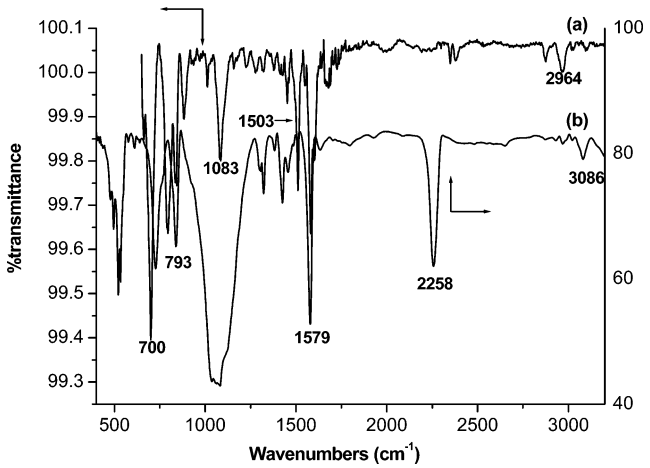

Figure 6. Comparison between the IR-RAS spectrum of **Fe+1** (a) and the KBr pellet IR of **D1** (b).

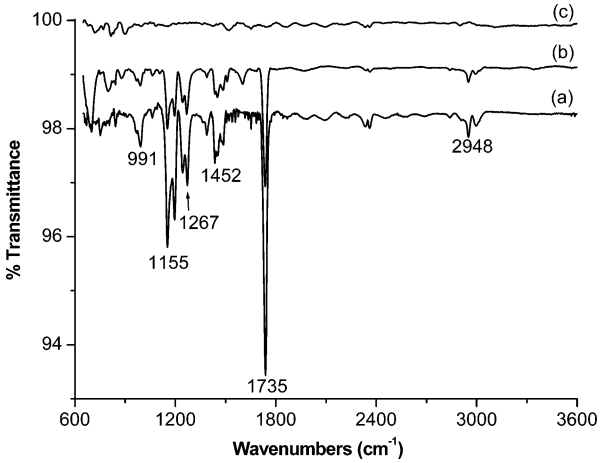

Figure 7. IR-RAS spectra of (a) **Fe+1+PMMA*** (experiment 4, Table 1), (b) **Fe+1+PMMA** (experiment 5, Table 1), and (c) **Fe+1** after incubation in PMMA (as prepared in experiment 4, Table 1) solution and subsequent solvent rinse.

In the case of PBA, similar features were observed for **Fe+1+PBA*** and the use of the sacrificial initiator gave the same trends as with surface-initiated PMMA brushes.

The possible existence of physisorbed polymer chains was investigated with electrochemically modified iron disks (**Fe+1**) that were heated for 4 h in a PMMA ($\bar{M}_n$ = 19 300 g/mol; $\bar{M}_w/\bar{M}_n$ = 1.16) solution in toluene at 90 °C in the absence of any sacrificial initiator and copper chloride. These experimental conditions (solvent and temperature) were chosen because they are similar to the protocol adopted for surface-initiated ATRP in this work. After five rinsings, for 5 min in dichloromethane under sonication, an IR-RAS analysis of the iron disks (Figure 7c) did not show any characteristic signal from PMMA,

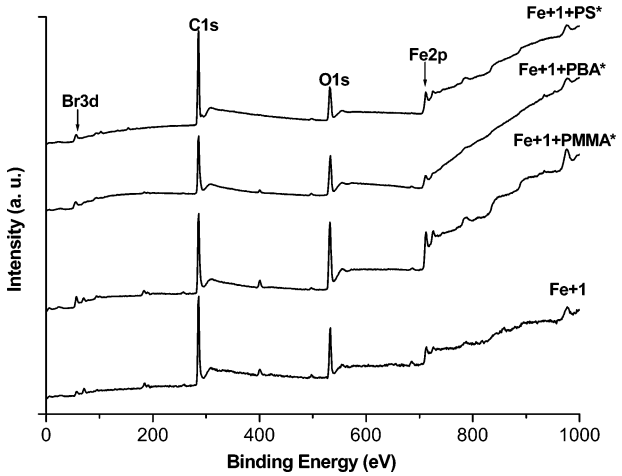

Figure 8. XPS survey scans of **Fe**+**1**, **Fe**+**1**+**PMMA*** (experiment 4, Table 1), **Fe**+**1**+**PBA*** (experiment 2, Table 1), and **Fe**+**1**+**PS*** (experiment 1, Table 1).

Table 2. Surface Chemical Compositions of Iron and Modified Iron Plates as Determined by XPS

	C	N	O	Fe	Cu	Br	Cl	F
Fe	30.6	0.51	50.4	18.6				
Fe+**1**	57.9	1.6	22.9	3.5	0.0	1.1	0.0	13
Fe+**1**+**PMMA**	72.0		27.7		0.07	traces	0.25	
Fe+**1**+**PMMA***	62.3	1.7	27.8	0.9	0.6	1.5	4.2	1.1
Fe+**1**+**PBA**	70.6	2.14	20.5	2.03	1.52	2.35	0.50	0.37
Fe+**1**+**PBA***	72.3	1.89	21.3	2.33	0.30	0.51	0.23	0.58
Fe+**1**+**PS***	81.8	0.31	14.4	3.01		0.08	0.16	0.24

indicating the absence of merely physisorbed polymers. It is noteworthy that, after three solvent rinsings, the supernatant did not exhibit any characteristic features of the leached polymer.

Figure 8 shows the XPS survey scans of **Fe**+**1**, **Fe**+**1**+**PMMA***, **Fe**+**1**+**PBA***, and **Fe**+**1**+**PS***. The main peaks Br(3d), C(1s), O(1s), and Fe($2p_{3/2}$) are centered at 71, 285, 530, and 707 eV, respectively. When PMMA, PBA, and PS brushes are grown from **Fe**+**1**, the slope of the spectral background beyond the Fe(2p) doublet gets steeper, an indication of inelastically scattered iron photoelectrons due to the grafted polymer brushes.

Table 2 presents the surface compositions of **Fe**, **Fe**+**1**, **Fe**+**1**+**PMMA**, **Fe**+**1**+**PBA**, and **Fe**+**1**+**PS** obtained by XPS.

The iron content in Fe is quite low due to the activation of the iron surface as a result of thorough polishing and cleaning. It should be noted that iron has not been argon-sputtered before XPS analysis, hence, its apparent high carbon content.

Following polymer grafting, the iron content significantly decreases from 18.6 down to 0.9−3.5%, and conversely the carbon atom % increases from 30.6% and levels off at 81.8% for PS brushes. Despite the significant changes in the surface compositions resulting from polymer grafting, the detection of iron, though at a low extent, is an indication of rather thin (<5−10 nm, which is the analysis depth of XPS) or inhomogeneous organic coatings.

Using the well-known relationship established by Kirste et al.,[45] it is possible to estimate R_g, the radius of gyration of the polymers in the vitreous state [$R_g = (0.096\mathrm{MW}^{0.98})^{1/2}$ Å]. Assuming that the MWs in the bulk solution and at the surface are the same, R_g = 4.2, 4.5, and 6.8 nm for PMMA*, PBA*, and PS* brushes, respectively. It follows that the diameters of gyration match the analysis depth in XPS (around 10 nm). For coatings in the 8−13-nm range, the substrate can be more or less completely screened.

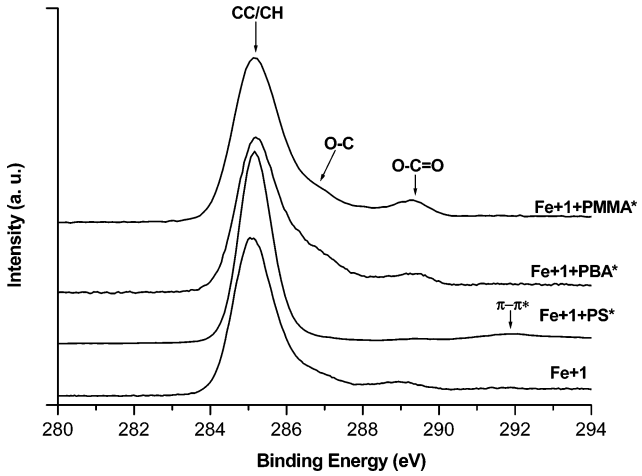

Figure 9. High-resolution C(1s) regions of **Fe**+**1**, **Fe**+**1**+**PMMA*** (experiment 4, Table 1), **Fe**+**1**+**PBA*** (experiment 2, Table 1), and **Fe**+**1**+**PS*** (experiment 1, Table 1).

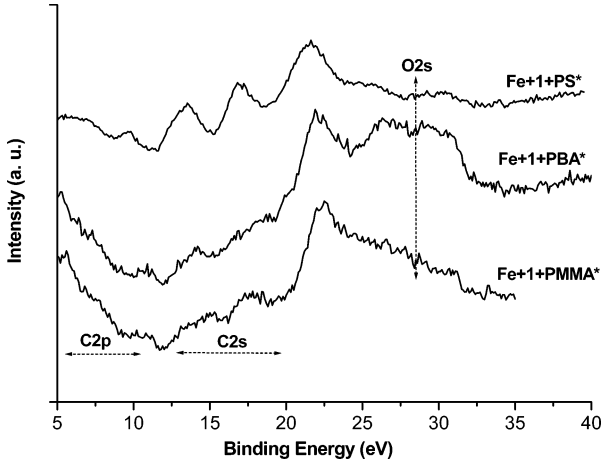

Figure 10. Valence band spectra of **Fe**+**1**+**PMMA*** (experiment 4, Table 1), **Fe**+**1**+**PBA*** (experiment 2, Table 1), and **Fe**+**1**+**PS*** (experiment 1, Table 1).

The detection of iron Fe(2p) core electrons (sampling depth ca. 9 nm) suggests that the lateral heterogeneity of the polymer coating thickness or incomplete coverage cannot be excluded (see AFM section).

The decreasing trend of the C/O atomic ratio is **Fe**+**1**+**PMMA*** (2.24) < **Fe**+**1**+**PMMA** (2.6) < **Fe**+**1**+**PBA*** (3.4) ∼ **Fe**+**1**+**PBA** (3.44). The C/O ratios between brackets match the theoretical values of 2.5 and 3.5 for bulk thick PMMA and PBA. At this stage, it is difficult to interpret the subtle difference in the C/O ratios obtained for these polymer brushes obtained in the presence or absence of the sacrificial initiator.

For **Fe**+**1**+**PS***, the C/O ratio is 27.2, far exceeding those of PMMA and PBA brushes since PS is free from oxygen.

For the uncoated and polymer-coated **Fe**+**1** surfaces, bromine reflects the presence of the −CH(CH_3)−Br moiety in the initiator and C−Br bonds in the polymer chain ends. Chlorine is detected by its Cl(2p) core−electron peak at ∼200 ± 0.5 eV for polymer-coated surfaces. This binding energy corresponds to C−Cl bonds, an indication that the polymeric chains are also terminated by a chlorine atom as in Scheme 2. The Cl/Br ratio is higher than 2 for the PS and PMMA brushes and in the 0.2−0.5 range for the PBA grafts. However, at this stage, one can certainly not

(45) Kirste, R. G.; Kruse, W. A.; Ibel, K. *Polymer* **1975**, *16*, 120.

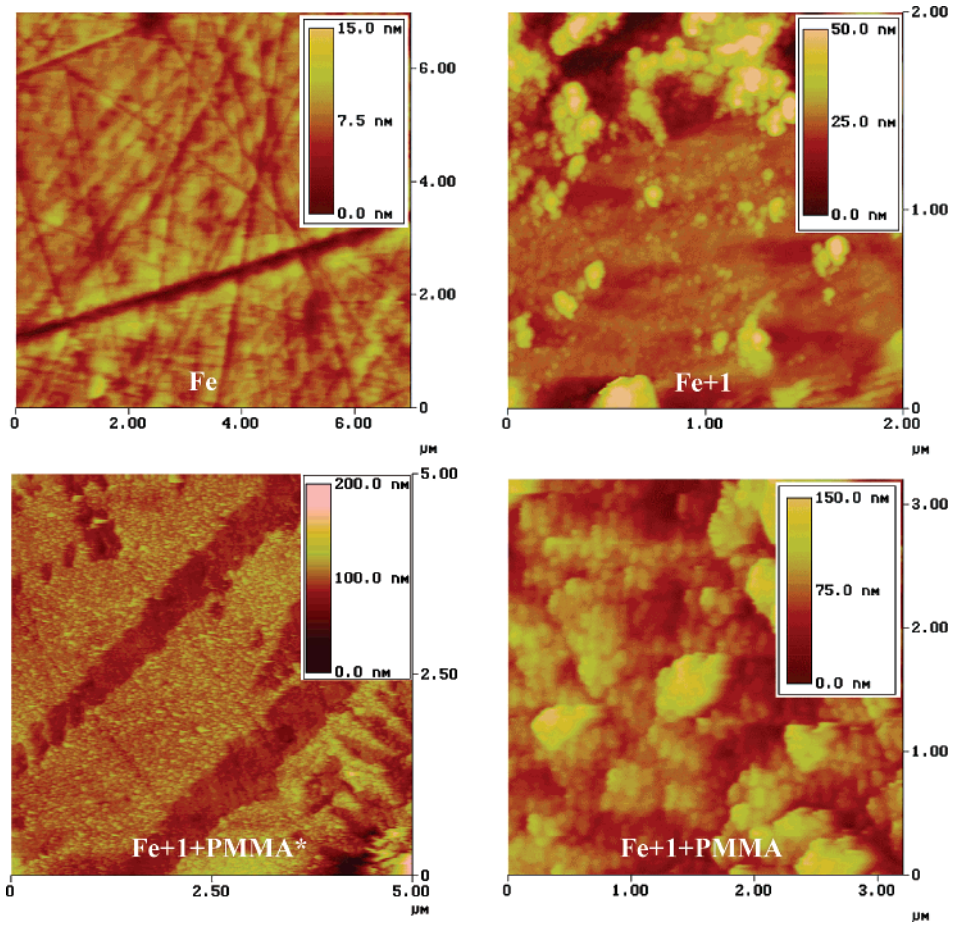

Figure 11. AFM images of **Fe**, **Fe**+**1**, **Fe**+**1**+**PMMA** (experiment 5, Table 1) and **Fe**+**1**+**PMMA*** (experiment 6, Table 1).

draw a general conclusion on the extent of chlorine and bromine at the terminus of the polymer brushes grown from the grafted diazonium salts.

Table 2 reports also the contributions to nitrogen [N(1s) centered at 401 eV] and fluorine (centered at 685 eV); these elements are due to traces of supporting electrolytes which have not been completely removed despite thorough rinsing. Moreover, copper is invariably detected, though at a negligibly small concentration.

The high-resolution C(1s) peaks from **Fe**+**1**, **Fe**+**1**+**PMMA***, **Fe**+**1**+**PBA***, and **Fe**+**1**+**PS*** are shown in Figure 9.

Fe+**1** exhibits a very weak feature centered at 291.5 eV due to a $\pi \rightarrow \pi^*$ shake-up satellite, which is a fingerprint of the aromatic, brominated species electrografted onto iron.

In the case of **Fe**+**1**+**PS***, the C(1s) peak has a main sharp peak at 285 eV and exhibits the characteristic shake-up satellite centered at ~291.5 eV due to the aromatic phenyl pendent groups.

For **Fe**+**1**+**PMMA***, the C(1s) region exhibits a prominent second maximum centered at 289 eV, which is assigned to the ester carbon atom. This is also the case for **Fe**+**1**+**PBA***, however, at a lesser extent since PBA has a higher C−C/C−H contribution. Actually the ratio between the components at 285 and 289 eV [C(1s)(CC/CH)/C(1s)(O−C=O) intensity ratio] is clearly higher for **Fe**+**1**+**PBA*,** which conforms to the known chemical structure of the grafted polymers.

It is clear that the C(1s) structures discussed above are in line with the nature of the polymer brushes grown from **Fe**+**1**. However, another elegant way to confirm the nature of the grafted polymers is to consider the valence bands in the 0−40 eV XPS spectral region. The valence band can actually be used as a fingerprint for a given polymer.

Figure 10 depicts the valence band spectra of **Fe**+**1**+**PMMA***, **Fe**+**1**+**PBA***, and **Fe**+**1**+**PS***. The complex structures of the C(2p) (5−12 eV), C(2s) (12−22 eV), and O(2s) (26−30 eV) features of the grafted polymers conform remarkably well with those published for spin-cast PMMA,[46] PS,[46] and PBA.[47] In the case of **Fe**+**1**+**PS***, O(2s) is due to the oxides, whereas the O(2s) region from **Fe**+**1**+**PBA*** has a structure comparable to that of **Fe**+**1**+**PMMA***.

The morphology of the polymer brushes was observed by AFM. Figure 11 shows that the morphology of the polymer-modified surfaces varies markedly from that of a clean iron surface or that of **Fe**+**1**. First, the change from **Fe** to **Fe**+**1** results in an increase in the maximum height (from 15 to 50 nm, respectively) and the average roughness (4.5 and 7.3 nm, respectively). After the surface-initiated ATRP of MMA, **Fe**+**1**+**PMMA** has a height up to 150 nm, which can reach 200 nm if PEBr is used as a sacrificial initiator (**Fe**+**1**+**PMMA***). However, while the brushes in **Fe**+**1**+**PMMA** may be "built" on the protruding features of the initiator layer and result in a cauliflower structure, the **Fe**+**1**+**PMMA*** exhibits a very compact structure with a few submicrometer-sized defects.

Preliminary wettability testing of the **Fe**+**1**+**PMMA*** and **Fe**+**1**+**PS*** was assessed by the sessile drop method using water as the reference liquid. The very low average

(46) Beamson, G., Briggs, D., Eds. *High Resolution XPS of Organic Polymers. The Scienta ESCA300 Database*; John Wiley: Chichester, 1992.

(47) Clark, D. T. In *Handbook of X-ray and ultraviolet photoelectron spectroscopy*; Briggs, D., Ed.; Heyden: London, 1977; Chapter 6, p 245.

roughness of the specimens is assumed not to affect the wettability measurements. The water contact angle was found to be 70.3 ± 2.1 and $88.1 \pm 2.0°$ for **Fe**+**1**+**PMMA*** and **Fe**+**1**+**PS***, respectively. The PS thin film grown from the iron surface appears significantly more hydrophobic than PMMA grown by the same approach, a result that is in line with the published water contact angle data for sheets of PMMA (64.3 ± 1.8 °)[48] and PS (80°).[49]

4. Conclusion

To our knowledge this is the first attempt to graft polymers by ATRP from metallic surfaces modified by the electrochemical reduction of a brominated aryl diazonium salt BF_4^-, $^+N_2-C_6H_4-CH(CH_3)-Br$ (**D1**). The grafted organic species $-C_6H_4-CH(CH_3)-Br$ was found to be very effective in initiating ATRP of MMA, BA, and styrene at the surface of iron. The PMMA, PBA, and PS overlayers were characterized by XPS, IR-RAS, AFM, and contact angle measurements. The combination of IR-RAS and XPS allowed detection of elemental markers and/or characteristic functional groups from the underlying electrochemically pretreated iron surfaces and from the grafted polymers. More importantly, the investigation of the XPS-excited valence band of the polymer-coated iron surfaces correlated remarkably well with the expected nature of the grafted polymers.

The polymer morphology studies of AFM emphasize the role of the sacrificial initiator in producing compact polymer overlayers grafted from the surface.

Simple wettability assessment of the polymer-modified surfaces using water drops showed that grafted PS is more hydrophobic than the grafted PMMA chains overlayer, which is consistent with published data on conventional PS and PMMA sheets.

This novel approach combining electrochemical attachment of initiators and ATRP adds another brick in the potential application of diazonium salts and also opens up new possibilities for graft polymerization from conductive substrates.

Acknowledgment. The authors wish to thank the French Ministry of Higher Education (FMHE) and the Conseil Régional d'Ile-de-France for financial support through the ACI Surfaces-Interfaces scheme n*o*. S43-01 and the SESAME 2000 project. T.M. gratefully acknowledges the FMHE for the provision of a studentship. Dr T. Basinka and Prof. S. Slomkowski (Center of Molecular and Macromolecular Studies, Łódź, Poland) are gratefully acknowledged for their assistance with wettability measurements.

LA046912M

(48) McCafferty, E.; Whightman, J. P. *J. Adhes. Sci. Technol.* **1999**, *13*, 1415.

(49) Gallardo-Moreno, A. M.; González-Martín, M. L.; Pérez-Giraldo, C.; Garduño, E.; Bruque, J. M.; Gómez-García, A. C. *Appl. Environ. Microbiol.* **2002**, *65*, 2610.